A PHOTOMETRIC TECHNIQUE FOR DETERMINING PLANETARY SLOPES FROM ORBITAL PHOTOGRAPHS

CONTRIBUTIONS TO ASTROGEOLOGY

Prepared on behalf of the National Aeronautics and Space Administration

GEOLOGICAL SURVEY PROFESSIONAL PAPER 812-A

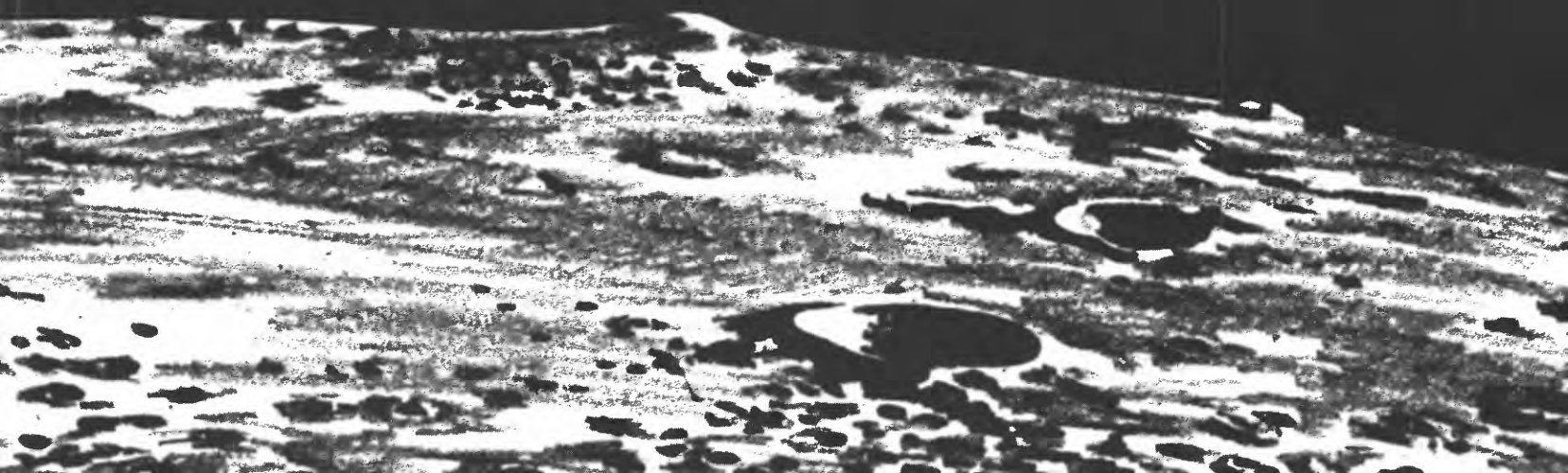

A Photometric Technique for Determining Planetary Slopes From Orbital Photographs

By W. J. BONNER *and* R. A. SCHMALL

CONTRIBUTIONS TO ASTROGEOLOGY

GEOLOGICAL SURVEY PROFESSIONAL PAPER 812-A

Prepared on behalf of the National Aeronautics and Space Administration

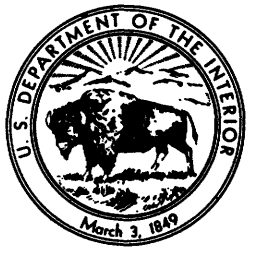

A closed form, general solution for photometric slope determination has been derived by use of vector mathematics. The technique can be applied equally well to vertical and to oblique photography

UNITED STATES GOVERNMENT PRINTING OFFICE, WASHINGTON : 1973

UNITED STATES DEPARTMENT OF THE INTERIOR

ROGERS C. B. MORTON, *Secretary*

GEOLOGICAL SURVEY

V. E. McKelvey, *Director*

Library of Congress catalog-card No. 73-600144

For sale by the Superintendent of Documents, U.S. Government Printing Office
Washington, D.C. 20402 – Price 40 cents (paper cover)
Stock Number 2401-02409

CONTENTS

ILLUSTRATIONS

SYMBOLOGY

Greek Symbols

α Brightness longitude.
λ Longitude coordinate on the lunar surface.
λ_o Longitude of the optic-axis intercept at lunar surface ($\lambda_o = \lambda_\tau$).
λ_τ Longitude of a point north of optic-axis intercept.
λ_s Longitude of the spacecraft.
$\lambda_\odot$ Longitude of the subsolar point.
β Latitude coordinate on the lunar surface.
β_o Latitude of the optic-axis intercept at lunar surface ($\beta_o = \beta_\tau$).
β_τ Latitude of a point north of optic-axis intercept.
β_s Latitude of the spacecraft.
$\beta_\odot$ Latitude of the subsolar point.
Φ Photometric function.
ψ Slope of the lunar surface measured in the phase plane.
ξ North deviation angle in the image plane.
η Coordinate on the lunar surface (positive toward the east).
η' Image-plane coordinate of the lunar surface.
ζ Coordinate on the lunar surface (positive toward the north).
ζ' Image-plane coordinate of a point on the lunar surface.
ω Angle between the mean lunar surface and the $\hat{e}_{z'}$ direction.
τ Point due north of optic-axis intercept (O).

Vectors

$\hat{e}$ Unit vectors defining a coordinate system.
$\hat{e}_1$ Base vector in the X or $(\eta+\zeta)$ direction.
$\hat{e}_2$ Base vector in Y or $(\eta+\zeta)$ direction.
$\hat{e}_3$ Base vector in the Z direction.
$\hat{e}_z$ Base vector in the Z direction.
$\bar{v}$ Vector.
$\bar{v}_o$ Vector from the moon's center to the optic-axis intercept.
$\bar{v}_\odot$ Vector from the moon's center to the subsolar point.
$\bar{v}_s$ Vector from the moon's center to the spacecraft.
$\bar{v}_p$ Vector from the moon's center to an arbitrary point on the lunar surface.
$\bar{v}_{ps}$ Vector from the arbitrary point p to the spacecraft.
$\hat{v}$ Unit vector as defined above.
$\hat{v}_o$ Unit vector as defined above.
$\hat{v}_\odot$ Unit vector as defined above.
$\hat{v}_s$ Unit vector as defined above.
$\hat{v}_p$ Unit vector as defined above.
$\hat{v}_{ps}$ Unit vector as defined above.
$\hat{v}_t$ Unit vector tangent to the local surface in the phase plane (also the slope of the lunar surface).
x_i Vector component in the direction of $\hat{e}_i$ vector, where i can take the value 1, 2, or 3.

Coordinates

X, Y, Z Lunar-centered coordinates:
X is through the mean libration center.
Z is north pointing (collinear with the axis of rotation).
Y completes the right-hand system.
Z Vertical coordinate on the lunar surface.
Z' Image-plane coordinate along the optic axis.
η, ζ, Z Moon-surface coordinates.
η', ζ', Z' Image-plane coordinates.

Other Symbols

A Altitude of the spacecraft above the lunar surface.
E Emitted ray (vector) to the camera.
f Focal length of the lens.
g Phase angle.
I Incident ray (vector) from the sun.
m Magnification factor.
R_m Radius of moon.
R_s Slant range along optic axis to optic-axis intercept.
S Spacecraft.
O Optic-axis intercept with the lunar surface.
SS Subspacecraft point on lunar surface.
T_{ij} Coordinate transformation matrix.

A PHOTOMETRIC TECHNIQUE FOR DETERMINING PLANETARY SLOPES FROM ORBITAL PHOTOGRAPHS

By W. J. BONNER and R. A. SCHMALL

ABSTRACT

Interest has been recurrent in applying photoclinometry (photometric technique for slope determination) to determine lunar slopes and heights where stereoscopic coverage was not available. Some scientists involved in the planetary program foresee the eventual application of the technique to such planets as Mars. As a result, a new approach to the problem by exclusive use of vector mathematics has been developed. The solution is generalized and can be applied equally well to extract slope information from either vertical or oblique photography. A summary of the procedure used for computing the slope is given for use in adapting the technique to computer programing.

INTRODUCTION

Photoclinometry is the process of relating the measured scene brightness, the viewing and lighting geometry, and the photometric function of a surface to obtain slope information. Historically, the technique was developed by van Diggelen (1951) to study mare ridges. Dale (1962) extended the technique to a generalized study of the topography of the maria. Wilhelms (1963) refined the technique and was first to apply it successfully to other types of lunar terrain. McCauley (1965) expanded the work to produce a detailed quantitative terrain map of the lunar equatorial belt. Finally, Watson (1968) established a rigorous mathematical foundation for the process and extended the technique to an analysis of normal photography from spacecraft imagery. The present paper expands the work to a generalized solution for determining roughness of terrain from spacecraft imagery.

The method is based on the assumption that the brightness of an element of the lunar surface is a function of the normal albedo, one component of the surface, and the sun's angle of elevation. Normal albedo is defined as the ratio of the emergent light to the incident light observed at zero phase angle. If the point-by-point variation of the normal albedo on the lunar surface is eliminated, the brightness of an element then depends only on the slope and the sun's angle of elevation, which are expressible as differences in lunar longitude near the equator. Figure 1 is an illustration of the relationship. The figure gives a polar view of the moon. The surface elements P and Q have the same albedo, and as a result of their similar angular relationship to the sun, they have the same brightness.

The angles POQ and DPE are equal, and the angle DPE is equal to the angle ABC, which is the east-west component of the slope for the element at P. The angle ABC can be expressed in terms of the difference in lunar longitude between the elements P and Q, or the difference in the sun's angle of elevation for measurements made near the equator. Thus, if two surface elements, separated in an east-west direction, have the same albedo and the same measured brightness, the slope of the surface at P is equal to the difference in lunar longitude or the difference in the angle of sun elevation between the elements (McCauley, 1965). Stated another way, if the brightness of the ridge at P is equal to the brightness of the sphere at a given distance from P (for example, Q), then the slope of the surface at P with respect to the sphere at P is equal to the angle $\psi = POQ$. The same is

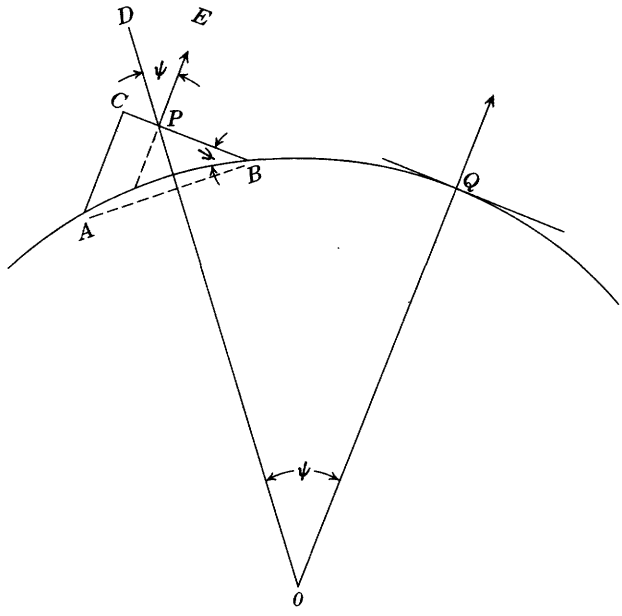

FIGURE 1.—Geometry for photometric slope determination. P and Q, surface elements.

true if P and Q are points of equal photographic transparency (van Diggelen, 1951).

PHOTOMETRIC FUNCTION

Use of the technique of photoclinometry to determine the roughness of the lunar surface requires that the reflection characteristics of the surface be taken into consideration, for the reliability of the data obtained from photoclinometry is primarily dependent on the precision to which the lunar photometric function is known.

From the work of Minnaert (1961) it is known that the functional form of the lunar photometric function has an interesting property (to within a precision of a few tens of percent): the brightness at any point, corrected for the normal albedo, is solely dependent on the brightness longitude and the phase angle.

Figure 2 represents the intersection of the phase plane with the lunar surface. The figure shows the path of an incident ray from the sun (I) and the ray emitted to the spacecraft—the emergent ray (E). The angle between the incident and emergent rays, measured in the plane containing both rays, is called the phase angle, g. Note that when the plane is tilted about the surface point, the phase angle remains constant. The angle measured in the phase plane between the emergent ray and the normal to the surface is defined as the brightness longitude, α. (The brightness longitude is defined positive when the projection of the normal into the phase plane is on the opposite side of the observer line from the location of the sun line, and negative when the projection lies between them—the only two possibilities.)

If the plane is rotated about the line of intersection with the surface, the brightness longitude remains constant. However, if the plane is tilted along an axis at a right angle to the line of intersection, the brightness longitude varies. Thus, the brightness at any point is a function of the slope component in the phase plane, the normal albedo, and the phase angle (Watson, 1968).

According to Watson (1968), two accepted photometric functions have been derived from earth-based observations. The first is that of Hapke (1963, 1966), which was derived by parametric fitting from theoretical considerations of a scattering model of the lunar surface. The second photometric function is based entirely on lunar photographic data and was derived entirely empirically by Herriman, Washburn, and Willingham (1963) and was later revised by Willingham (1964). Figure 3 shows the two functions in graphical form. In the figure, brightness is plotted as a function of the brightness longitude, α, and the phase angle, g. As Watson (1968) pointed out, a major limitation in constructing a photometric function from terrestrial observations is that a particular lunar feature cannot be observed for a wide variety of earth-angle observations. The

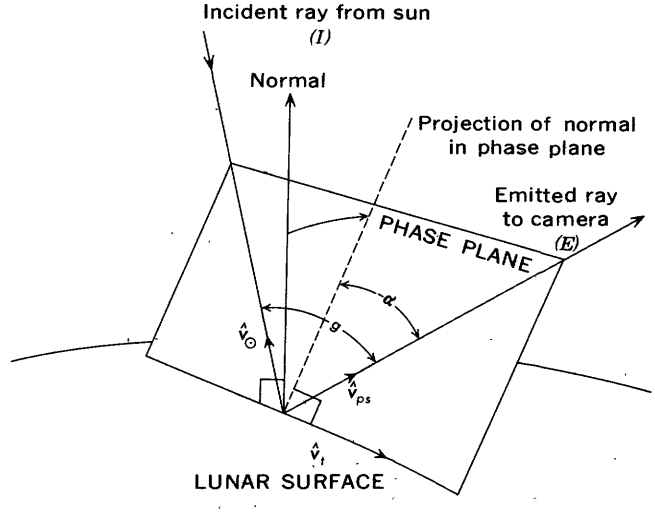

FIGURE 2.—Phase-plane nomenclature depicting relations between brightness longitude (α) and phase angle (g).

problem is primarily that a libration in longitude of the moon of only ±8° makes data on a single feature available only over a narrow range of brightness longitudes. Another serious problem with obtaining the photometric function terrestrially is that scientific data are not available on its dispersion characteristics. R. L. Wildey (unpub. data) has devised an ingenious method for determining these dispersion properties, and it is hoped that this experiment will eventually be carried out.

DERIVATION OF COORDINATE SYSTEMS

In presenting this mathematical process of using photometric data to evaluate the slope, it is

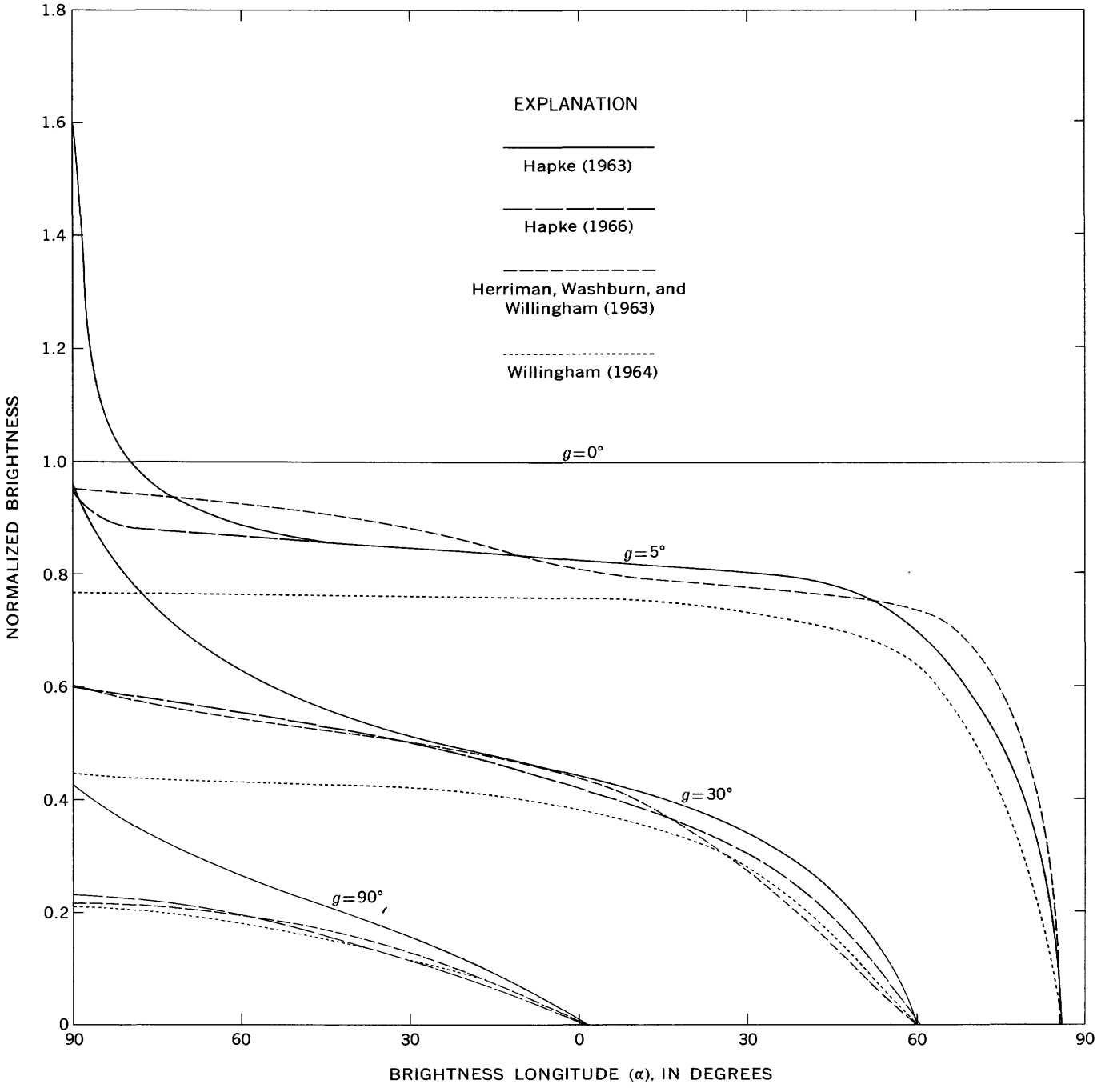

FIGURE 3.—Lunar photometric functions. Brightness (normalized to unity at $g=0°$) is plotted as a function of brightness longitude (α) and phase angle (g). From Watson (1968).

convenient to define several coordinate systems. To minimize confusion, each coordinate system will be defined when it is needed in the mathematical development. In addition, the nomenclature has been selected to eliminate ambiguity.

The physical phenomenon that forms the basis for photoclinometric terrain analysis is that a functional relationship exists between the brightness, the phase angle, and the brightness longitude. Thus, if any two of these quantities are known, the third is also known. Figure 2 depicts the phase plane geometry. As shown in the figure, if the phase angle g and brightness Φ are known, the brightness longitude α can be evaluated. The scene brightness can be determined by relating the measured film density to brightness through the film H and D curve. The phase angle is obtained from the position geometry of the point of interest on the film, the lunar time, and the season. The problem is thus reduced to evaluating g from the image information to permit the evaluation of α. Then α and the image information are used to evaluate the slope of the surface.

To determine the phase angle, use was made of a coordinate system whose lines intercept at the center of the moon. Figure 4 shows this moon-center coordinate system. The Z axis goes through the north pole, the X axis is located through the mean libration plane, and the Y axis completes a right-handed orthogonal coordinate system. (See fig. 5.)

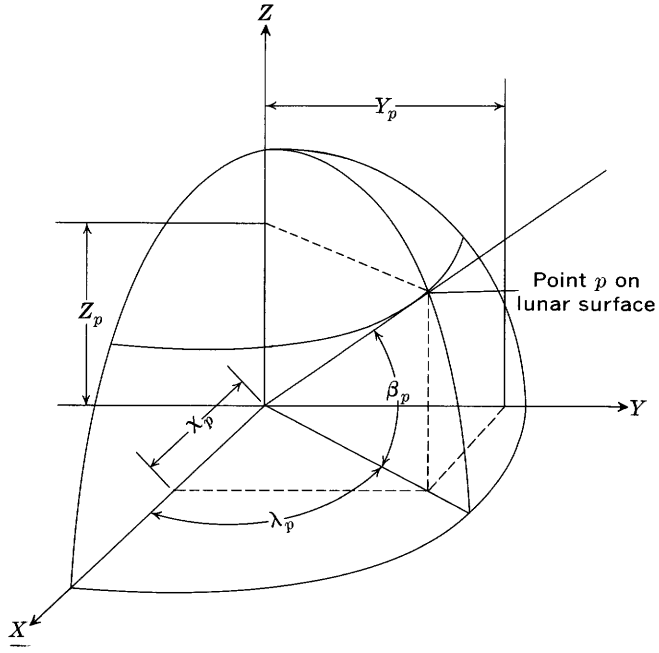

FIGURE 4. – Moon-center coordinate system.

Figure 6 illustrates the geometry of the phase plane projected onto the plane containing the origin (center of the moon), the subsolar point, and an arbitrary point of interest, p, on the lunar surface.

The following subscripts are used to denote position vectors (these vectors originate at the origin of the coordinate system):

Subscript	*Position vector*
$\odot$	Subsolar point (on the lunar surface).
p	Arbitrary point (on the lunar surface).
s	Spacecraft (at an altitude A above lunar surface).

In addition to the above notation, an overscribed caret represents a unit vector and an overscribed line denotes a vector; thus

$\hat{v}$ = unit vector.

$\bar{v}$ = vector.

From figure 6, the phase angle is found from the vector relationships

$$\cos g = \hat{v}_{\odot} \cdot \hat{v}_{ps}, \tag{1}$$

where

$$\hat{v}_{\odot} = \frac{\bar{v}_{\odot}}{R_m}$$

Also,

$$\hat{v}_{ps} = \frac{\bar{v}_{ps}}{|\bar{v}_{ps}|} \tag{2}$$

and

$$\bar{v}_{ps} = \bar{v}_s - \bar{v}_p.$$

From figure 4, the latitude and longitude are used to locate positions on the lunar surface. The vector representation in rectangular coordinates is

$$\hat{v}_p = \cos \beta_p \cos \lambda_p \, \hat{i} + \cos \beta_p \sin \lambda_p \, \hat{j} + \sin \beta_p \, \hat{k}, \tag{3}$$

where $\hat{i}$, $\hat{j}$, and $\hat{k}$ are unit vectors in the X, Y, and Z directions.

Similarly,

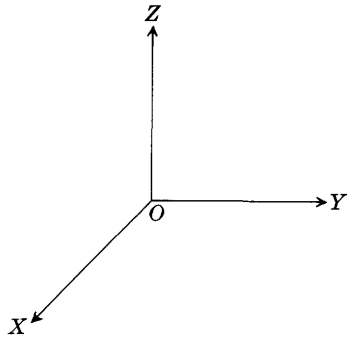

FIGURE 5.—Right-handed orthogonal system. A right-handed system means that if one rotates OX into OY, then OZ will lie in the direction in which a right-hand screw would advance. The lines OX, OY, OZ indicate the positive directions of the coordinate axis.

$$\hat{v}_\odot = \cos\beta_\odot \cos\lambda_\odot \hat{i} + \cos\beta_\odot \sin\lambda_\odot \hat{j} + \sin\beta_\odot \hat{k} \quad (4)$$

$$\hat{v}_s = \cos\beta_s \cos\lambda_s \hat{i} + \cos\beta_s \sin\lambda_s \hat{j} + \sin\beta_s \hat{k}. \quad (5)$$

We note that

$$\bar{v}_{ps} = \bar{v}_s - \bar{v}_p = (R_m + A)\ \hat{v}_s - R_m\, \hat{v}_p. \quad (6)$$

Substituting equations 3 and 5 in equation 6, we obtain

$$\bar{v}_{ps} = R_m \left\{ \left[\left(1 + \frac{A}{R_m}\right) \cos\beta_s \cos\lambda_s - \cos\beta_p \cos\lambda_p \right] \hat{i} \right.$$

$$+ \left[\left(1 + \frac{A}{R_m}\right) \cos\beta_s \sin\lambda_s - \cos\beta_p \sin\lambda_p \right] \hat{j}$$

$$\left. + \left[\left(1 + \frac{A}{R_m}\right) \sin\beta_s - \sin\beta_p \right] \hat{k} \right\} \quad (7)$$

Also,

$$|\bar{v}_{ps}| = |\bar{v}_s - \bar{v}_p|$$

$$\therefore |\bar{v}_{ps}| = R_m \left\{ \left[\left(1 + \frac{A}{R_m}\right) \cos\beta_s \cos\lambda_s - \cos\beta_p \cos\lambda_p \right]^2 \right.$$

$$+ \left[\left(1 + \frac{A}{R_m}\right) \cos\beta_s \sin\lambda_s - \cos\beta_p \sin\lambda_p \right]^2$$

$$\left. + \left[\left(1 + \frac{A}{R_m}\right) \sin\beta_s - \sin\beta_p \right]^2 \right\}^{1/2}$$

$$|\bar{v}_{ps}| = R_m \left\{ \left(1 + \frac{A}{R_m}\right)^2 + 1 - 2\left(1 + \frac{A}{R_m}\right) \right.$$

$$\left. [\cos\beta_s \cos\beta_p \cos(\lambda_s - \lambda_p) + \sin\beta_s \sin\beta_p] \right\}^{1/2} \quad (8)$$

Using equations 4, 7, 8 in 1, we now determine the phase angle.

$$\cos g = \frac{\bar{v}_{ps} \cdot \hat{v}_\odot}{|\bar{v}_{ps}|},$$

$$\therefore \cos g =$$

$$\frac{\left(1 + \frac{A}{R_m}\right) \left\{ [\cos\beta_\odot \cos\beta_s \cos(\lambda_s - \lambda_\odot) + \sin\beta_\odot \sin\beta_s] - [\cos\beta_\odot \cos\beta_p \cos(\lambda_p - \lambda_\odot) + \sin\beta_\odot \sin\beta_p] \right\}}{\left\{ \left(1 + \frac{A}{R_m}\right)^2 + 1 - 2\left(1 + \frac{A}{R_m}\right) [\cos\beta_s \cos\beta_p \cos(\lambda_s - \lambda_p) + \sin\beta_s \sin\beta_p] \right\}^{1/2}} \quad (9)$$

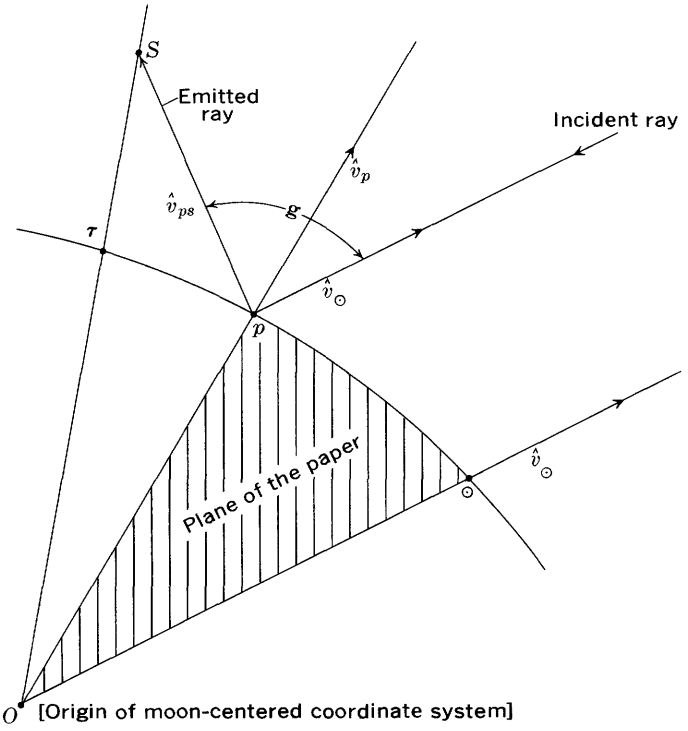

FIGURE 6.—Parameters for determining the phase angle g. p, arbitrary point on the lunar surface.

where

$\beta_\odot, \lambda_\odot$ are the latitude and longitude of the subsolar point.

β_s, λ_s are the latitude and longitude of the subspacecraft point, (also latitude and longitude of the spacecraft).

β_p, λ_p are the latitude and longitude of an arbitrary point of interest on the lunar surface.

R_m is the radius of the moon.

The quantities $\lambda_\odot, \beta_\odot, \lambda_s, \beta_s$ can all be determined from the mission support data. R_m is a constant over the area of interest, and β_p, λ_p can be determined from the location of R_m in the image plane. The method by which β_p, λ_p are determined will be discussed later.

Referring to figure 2 the vector $\hat{v}_t$ represents the local tangent. Therefore, the slope of $\hat{v}_t$ is the local slope of the terrain. Since $\hat{v}_p$ is a unit vector in the radial direction (that is, points to the local zenith, see fig. 6), the slope of the terrain can be found from the relationship

$$\cos(90-\psi) = \hat{v}_t \cdot \hat{v}_p, \tag{10}$$

where ψ = the slope of the terrain.

The unit vector $\hat{v}_t$ is determined as follows. By defining $\hat{v}_g$ as a unit vector normal to the phase plane, then

$$\hat{v}_g = \frac{\hat{v}_\odot \times \hat{v}_{ps}}{\sin g} = \frac{\hat{v}_\odot \times \hat{v}_t}{\sin(90-\alpha+g)}. \tag{11}$$

Also,

$$\frac{\hat{v}_\odot \times (\hat{v}_\odot \times \hat{v}_{ps})}{\sin g} = \frac{\hat{v}_\odot \times (\hat{v}_\odot \times \hat{v}_t)}{\sin(90-\alpha-g)}. \tag{12}$$

Expansion of equation 12 by means of the triple vector product identity yields

$$\frac{(\hat{v}_\odot \cdot \hat{v}_{ps})\,\hat{v}_\odot - (\hat{v}_\odot \cdot \hat{v}_\odot)\,\hat{v}_{ps}}{\sin g} = \frac{(\hat{v}_\odot \cdot \hat{v}_t)\,\hat{v}_\odot - (\hat{v}_\odot \cdot \hat{v}_\odot)\,\hat{v}_t}{\sin(90-\alpha-g)}. \tag{13}$$

Note that

$\hat{v}_\odot \cdot \hat{v}_{ps} = \cos g$ (which is equation 1)

$\hat{v}_\odot \cdot \hat{v}_\odot = 1$

$\hat{v}_\odot \cdot \hat{v}_t = \cos(90-\alpha+g) = -\sin(g-\alpha).$

Substituting the above set of equations into equation 13 and solving for $\hat{v}_t$, we obtain

$$\hat{v}_t = -\hat{v}_\odot[\sin(g-\alpha) + \cot g \cos(g-\alpha)] + \hat{v}_{ps}\left[\frac{\cos(g-\alpha)}{\sin g}\right]. \tag{14}$$

The slope of the terrain may now be determined from equation 10. We have

$$\sin\psi = \cos(90-\psi) = \hat{v}_p \cdot \hat{v}_t. \tag{15}$$

Substituting equation 14 into equation 15 we obtain

$$\sin\psi = -[\sin(g-\alpha) + \cot g \cos(g-\alpha)]\,\hat{v}_\odot \cdot \hat{v}_p + \left[\frac{\cos(g-\alpha)}{\sin g}\right]\hat{v}_{ps} \cdot \hat{v}_p. \tag{16}$$

From equations 3 and 4 we note

$$\hat{v}_\odot \cdot \hat{v}_p = \cos\beta_\odot \cos\beta_p \cos(\lambda_\odot - \lambda_p) + \sin\beta_\odot \sin\beta_p. \tag{17}$$

From equations 2 and 3 and 6 we have

$$\hat{v}_{ps} \cdot \hat{v}_p = \left[\frac{\left(1+\frac{A}{R_m}\right)\hat{v}_s - \hat{v}_p}{|\bar{v}_{ps}|/R_m}\right] \cdot \hat{v}_p = \frac{\left(1+\frac{A}{R_m}\right)\hat{v}_p \cdot \hat{v}_s - 1}{|\bar{v}_{ps}|/R_m}. \tag{18}$$

From equations 3 and 5 we have

$$\hat{v}_p \cdot \hat{v}_s = \cos\beta_p \cos\beta_s \cos(\lambda_s - \lambda_p) + \sin\beta_p \sin\beta_s. \tag{19}$$

Substitution of equations 8 and 19 in equation 18 yields

$$\hat{v}_{ps} \cdot \hat{v}_p =$$

$$\frac{\left\{\left[\left(1+\frac{A}{R_m}\right)\cos\beta_p \cos\beta_s \cos(\lambda_s-\lambda_p) + \sin\beta_p \sin\beta_s\right]-1\right\}}{\left\{\left(1+\frac{A}{R_m}\right)^2+1-2\left(1+\frac{A}{R_m}\right)\left[\cos\beta_s\cos\beta_p \cos(\lambda_s-\lambda_p)+\sin\beta_s\sin\beta_p\right]\right\}^{1/2}} \quad (20)$$

∴ The slope of the surface may be elevated by substituting equations 17 and 20 into equation 16. Note, however, that the quantities β_p and λ_p are still undetermined.

In order to evaluate β_p and λ_p a second coordinate system is now defined. Figure 7 defines a curvilinear coordinate system which is centered at the camera optic axis intercept with the surface. The coordinates η and ζ are curvilinear and coincide with lines on constant longitude (north pointing positive ζ) and constant latitude (east pointing positive η). The Z coordinate is in the direction of the local vertical with positive up. (Note that we are dealing with two different coordinate systems as defined in the nomenclature. Also note that this is the second instance that the letter Z has been used in defining a system coordinate.)

Assume that the distances involved are small compared to the moon's radius. Then the arbitrary point p can be approximated as follows:

$$\eta_p - \eta_o = R_m \cos\beta_o (\lambda_p - \lambda_o).$$

Also,

$$\zeta_p - \zeta_o = -R_m (\beta_p - \beta_o).$$

Rearranging the two equations and noting that η_o and ζ_o are defined as the center of the coordinate system and are therefore equal to zero, we have

$$\beta_p = \frac{\eta_p}{R_m \cos\beta_o} + \lambda_o \quad (21)$$

and

$$\lambda_p = \lambda_o - \frac{\zeta_p}{R_m}, \quad (22)$$

where β_o, λ_o = optic axis intercept with the lunar surface. Figure 8 represents the image plane coordinate system. The origin is located at the intersection of the optic axis with the image plane. In other words, η_o' and ζ_o' is the image of the optic axis intercept with the lunar surface. The third coordinate Z' is parallel to the optic axis and is positive in the direction toward the moon.

Figure 8 also defines the angle ξ. This angle is between the image north (the positive ζ' axis) and the image of north pointing β_o (the north-pointing longitude through the optic axis intercept with the lunar surface).

Therefore, if the η_p', ζ_p' coordinates of the image plane can be transformed into the η_p, ζ_p coordinates of the lunar surface, the local terrain slope can be evaluated as follows:

1. Equations 21 and 22 are evaluated for (β_p, λ_p).
2. With this information, equation 9 is evaluated for g.

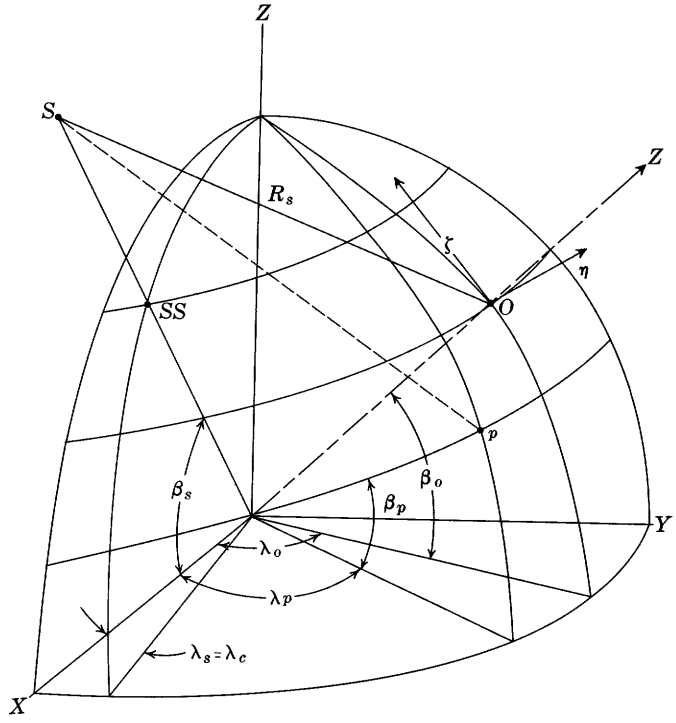

FIGURE 7.—Relationships between the moon-center coordinate system and the moon-surface coordinate system. p, arbitrary point.

3. α is now determined from the photometric function.
4. Using this information and equations 17 and 20 in equation 16, the slope can be determined.

The position vector $\bar{v}_{op}$ in the image plane coordinate system (η', ζ', Z') is

$$\bar{v}_{op} = m[\eta'_p \hat{e}_{\eta'} + \zeta'_p \hat{e}_{\zeta'} + Z'_p \hat{e}_{z'}], \tag{23}$$

where

m = magnification factor $= \dfrac{R_s}{f}$.

R_s = slant range from the camera to the optic axis intercept with the lunar surface.

f = camera focal length.

Equation 23 permits the evaluation of the vector, $\bar{v}_{op}$, in the image plane coordinates (that is, except for Z'_p which will be discussed later). Therefore, a transformation matrix between the lunar surface coordinate system and the image plane coordinate system will solve the problem.

Since a vector is an invariant, a vector $(\bar{v})$ may be represented in two coordinate systems. (Recall that an invariant is an expression involving the coefficients of an *algebraic function* which remains constant when a *transformation*, such as translation or rotation of coordinate axes, is made.)

$$\therefore \bar{v} = \sum_i x_i \hat{e}_i = \sum_j x'_j \hat{e}'_j,$$

where x_i is the vector component in the direction $\hat{e}_i$ and i can take the values 1, 2, or 3.

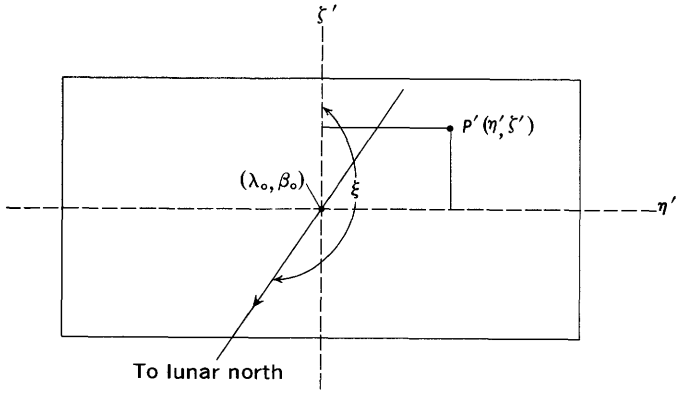

FIGURE 8.– Image-plane coordinate system and the definition of the angle ξ.

Dotting $\hat{e}_i$ into the above equation we obtain

$$\sum_i \hat{e}_i \cdot (x_i \hat{e}_i) = \sum_j \hat{e}_i \cdot (x'_j \hat{e}'_j). \tag{24}$$

Solving equation 24 for x_i and noting that $\hat{e}_i \cdot \hat{e}_i = 1$, we have

$$x_i = \sum_j (\hat{e}_i \cdot \hat{e}'_j) x_j = \sum_j T_{ij} x_j.$$

Solving the above equation for T_{ij}, we obtain

$$T_{ij} = \hat{e}_i \cdot \hat{e}'_j. \tag{25}$$

The elements of the matrix T_{ij} are the cosines of the angles between the coordinate axes. That is, T_{33} is the cosine of the angle between the Z and Z' axes, and T_{13} is the cosine of the angle between the η and Z' axes, and so forth.

The transformation matrix is now defined and some generalizations are possible with respect to equation 23. These are

1. The distance of concern on the lunar surface is small compared to the slant range.
2. The lunar surface is assumed to be flat over the distances involved.

In figure 9, the two coordinate systems under consideration have been drawn with a common origin. From this illustration the following can be seen:

$$\tan \omega = \frac{[(\hat{e}'_3 \times \hat{e}_3) \times \hat{e}'_3] \cdot (\eta'_p \hat{e}'_1 + \zeta'_p \hat{e}'_2)}{[\hat{e}_3 \times (\hat{e}'_3 \times \hat{e}_3)] \cdot (\eta'_p \hat{e}'_1 + \zeta'_p \hat{e}'_2 + Z'_p \hat{e}'_3)} \tag{26}$$

Expanding equation 26 using the triple vector-product identity (summary of the relationships used in this report given in Coburn (1955) and Kaplan (1959)), we obtain

$$\tan \omega = \frac{(\hat{e}_3 - T_{33} \hat{e}'_3) \cdot (\eta'_p \hat{e}'_1 + \zeta'_p \hat{e}'_2)}{(\hat{e}'_3 - T_{33} \hat{e}_3) \cdot (\eta'_p \hat{e}'_1 + \zeta'_p \hat{e}'_2 + Z'_p \hat{e}'_3)}, \tag{27}$$

where

$$T_{33} = \hat{e}'_3 \cdot \hat{e}_3.$$

Noting that $\hat{e}'_i \cdot \hat{e}'_j = 0$ for $i \neq j$ and performing the vector dot product, we have

$$\tan \omega = \frac{T_{31} \eta'_p + T_{32} \zeta'_p}{-T_{33}(T_{31} \eta'_p + T_{32} \zeta'_p + T_{33} Z'_p) + Z'_p}. \tag{28}$$

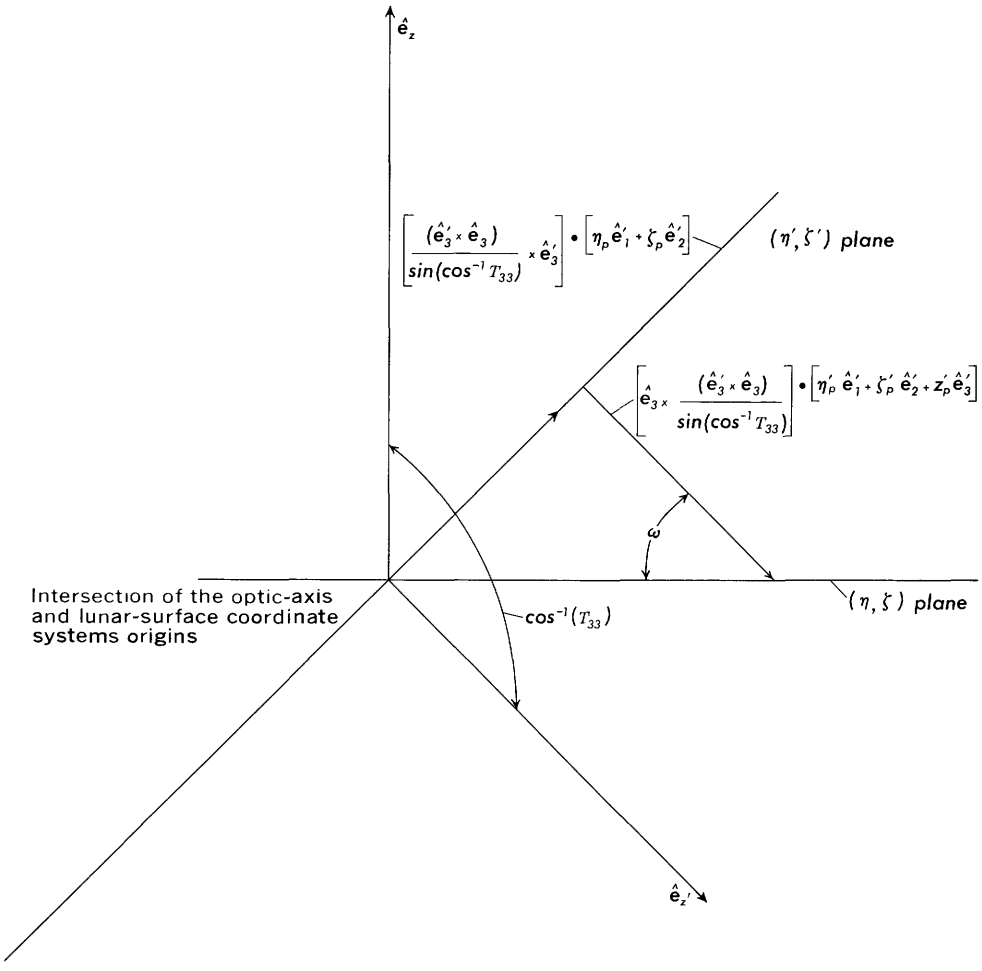

FIGURE 9.—Procedure for evaluating the third image plane coordinate Z'.

Note: The plane of the figure is the $\hat{e}_z - \hat{e}_{z'}$ plane.

From figure 9, we note

$$\tan \omega = \frac{\cos(\cos^{-1} T_{33} - 90)}{\sin(\cos^{-1} T_{33} - 90)} = \frac{-\sin(\cos^{-1} T_{33})}{\cos(\cos^{-1} T_{33})}$$

or

$$\tan \omega = -\frac{\sqrt{1 - T_{33}^2}}{T_{33}}. \tag{29}$$

Substituting equation 29 into equation 28 and solving for Z_p', we obtain

$$Z_p' = \frac{T_{33}(\sqrt{1 - T_{33}^2} - 1)\ (T_{31}\eta_p' + T_{32}\zeta_p')}{\sqrt{1 - T_{33}^2}\ (1 - T_{33}^2)}. \tag{30}$$

Let,

$$K = \frac{T_{33}(\sqrt{1 - T_{33}^2} - 1)}{\sqrt{1 - T_{33}^2}\ (1 - T_{33}^2)}.$$

It is now possible to evaluate η_p and ζ_p by knowing η_p' and ζ_p'.

$$\therefore \eta_p = m\ [T_{11}\eta_p' + T_{12}\zeta_p' + T_{13}Z_p'] \tag{31a}$$

$$\zeta_p = m\ [T_{21}\eta_p' + T_{22}\zeta_p' + T_{23}Z_p'] \tag{31b}$$

Substituting equation 30 into equation 31a and 31b, we obtain

$$\eta_p = m\ [(T_{11} + T_{13}KT_{31})\ \eta_p' + (T_{12} + T_{13}KT_{32})\ \zeta_p'] \tag{32}$$

$$\zeta_p = m\ [(T_{21} + T_{23}KT_{31})\ \eta_p' + (T_{22} + T_{23}KT_{32})\ \zeta_p] \tag{33}$$

Equations 32 and 33 can be substituted into equations 21 and 22 to obtain β_p, λ_p. β_p and λ_p can then be used to determine g in equation 9. With this information the brightness longitude (α) can be determined from the photometric function. And then

using equations 16, 17, and 20, the slope of the terrain can be determined. The last step remaining then is the evaluation of the transformation matrix (T_{ij}) which is determined in the following section.

COORDINATE TRANSFORMATION MATRIX

To facilitate the evaluation of the coefficients of the transformation matrix, this matrix will be evaluated in two steps. Recall that if three coordinate systems exist such that

$$x_i = \sum_j T'_{ij} x''_j$$

$$x_j = \sum_k T''_{jk} x'_k$$

then,

$$x_i = \sum_J T'_{ij} x''_j = \sum_{jk} T'_{ij} T''_{jk} x'_k = \sum_k T_{ik} x'_k, \tag{34}$$

where

$$T_{ik} = \sum_j T'_{ij} T''_{jk}.$$

Therefore, defining an image plane coordinate system (η', ζ', Z') such that $\xi = 0$ (see fig. 10) also defines a transformation matrix such that

$$x_i = \sum_i T_{ij} x_j, \tag{35}$$

where

$$x_1 = \eta,\ x_2 = \zeta,\ x_3 = Z'.$$

That is,

$$\eta = T'_{11}\eta'' + T'_{12}\zeta'' + T'_{13}Z' \tag{36a}$$

$$\zeta = T'_{21}\eta'' + T'_{22}\zeta'' + T'_{23}Z' \tag{36b}$$

$$Z = T'_{31}\eta'' + T'_{32}\zeta'' + T'_{33}Z'. \tag{36c}$$

Since $\xi = 0$, the ζ'', Z' and ζ axes lie in the same plane and the η'' axis is perpendicular to the ζ'' and Z' plane and is therefore perpendicular to the ζ axis; also

$$T'_{ij} = \hat{e}_i \cdot \hat{e}''_j$$

$$\therefore \hat{e}_\zeta \cdot \hat{e}''_\eta = \hat{e}_2 \cdot \hat{e}''_1 = 0 \tag{37a}$$

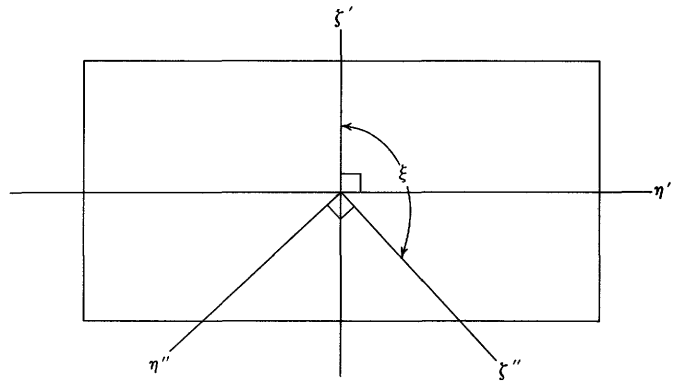

FIGURE 10.—Image-plane coordinate systems.

$$T'_{21} = 0. \tag{37b}$$

Now,

$$T'_{33} = \hat{e}_3 \cdot \hat{e}''_3 = \hat{e}_z \cdot \hat{e}'_z.$$

Referring to figure 11 and applying the law of cosines, we have

$$(A + R_m)^2 = R_s^2 + R_m^2 - 2R_m(R_s)T'_{33}.$$

Solving for T'_{33}, we obtain

$$T'_{33} = \frac{1}{2}\left[\frac{R_s}{R_m} - \frac{A}{R_s}\left(\frac{A}{R_m} + 2\right)\right]. \tag{38}$$

From figure 12, we note that

$$T'_{23} = \hat{e}'_z \cdot \hat{e}_\zeta = \lim_{\lambda_\tau \to \lambda_o} \frac{\bar{v}_{so} \cdot \bar{v}_{\tau o}}{|\bar{v}_{so}|\,|\bar{v}_{\tau o}|}, \tag{39}$$

where τ is defined as a point due north of O ($\lambda_\tau = \lambda_o$).

$$\bar{v}_{so} = \bar{v}_s - \bar{v}_o$$

$$\bar{v}_{\tau o} = \bar{v}_\tau - \bar{v}_o$$

NOTE.—Recall that single subscripted vectors refer to position vectors relative to the center of the moon.

As previously defined, we have

$$\bar{v}_o = R_m\,[\cos\beta_o \cos\lambda_o \hat{e}_x + \cos\beta_o \sin\lambda_o \hat{e}_y + \sin\beta_o \hat{e}_z]$$

$$\bar{v}_\tau = R_m\,[\cos\beta_\tau \cos\lambda_\tau \hat{e}_x + \cos\beta_\tau \sin\lambda_\tau \hat{e}_y + \sin\beta_\tau \hat{e}_z]$$

$$\bar{v}_s = (R_m + A)\,[\cos\beta_s \cos\lambda_s \hat{e}_x + \cos\beta_s \sin\lambda_s \hat{e}_y + \sin\beta_s \hat{e}_z]$$

$$\therefore \bar{v}_{so} = [(A+R_m)\cos\beta_s \cos\lambda_s - R_m \cos\beta_o \cos\lambda_o]\hat{e}_x + [(A+R_m)\cos\beta_s \sin\lambda_s - R_m \cos\beta_o \sin\lambda_o]\,\hat{e}_y + [(A+R_m)\sin\beta_s - R_m \sin\beta_o]\,\hat{e}_z \quad (40)$$

$$\bar{v}_{ro} = R_m\,[(\cos\beta_r - \cos\beta_o)\cos\lambda_o \hat{e}_x + (\cos\beta_r - \cos\beta_o)\sin\lambda_o \hat{e}_y + (\sin\beta_r - \sin\beta_o)\,\hat{e}_z] \quad (41)$$

Also

$$|\bar{v}_{so}| = R_s \quad (42)$$

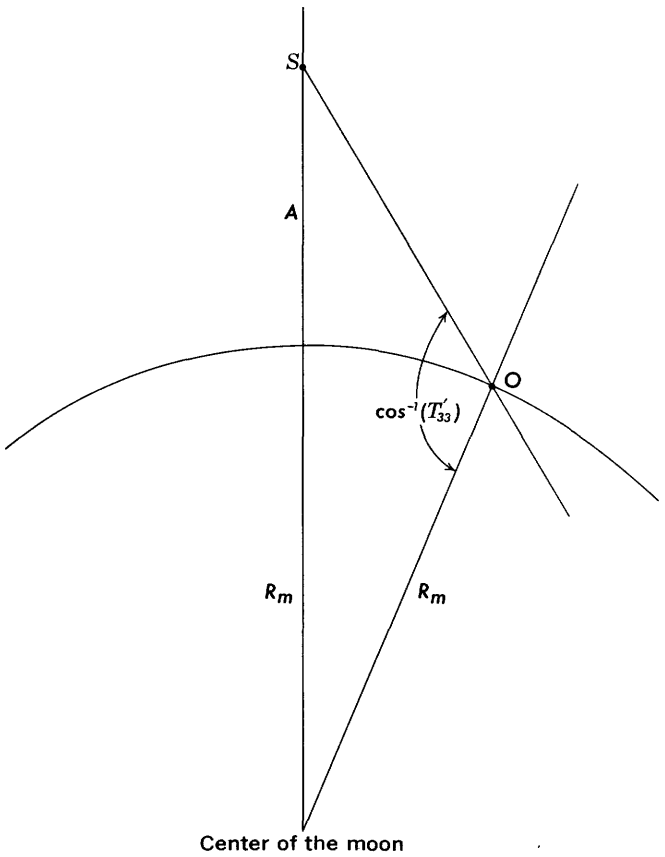

FIGURE 11.—Geometric quantities in the plane described by the points S, O, and the center of the moon.

$$|\bar{v}_{ro}| = R_m(\beta_r - \beta_o), \text{ for } (\beta_r - \beta_o) \text{ small.} \quad (43)$$

We note the following relationships

$$\beta_r \lim_{\rightarrow} \beta_o \cos(\beta_r - \beta_o) = 1$$

$$\beta_r \lim_{\rightarrow} \beta_o \sin(\beta_r - \beta_o) = \beta_r - \beta_o$$

$$\beta_r \lim_{\rightarrow} \beta_o (\cos\beta_r - \cos\beta_o) = \cos[\beta_o + (\beta_r - \beta_o)] - \cos\beta_o = \cos\beta_o \cos(\beta_r - \beta_o) - \sin\beta_o = \sin(\beta_r - \beta_o) - \cos\beta_o$$

that is,

$$\beta_r \lim_{\rightarrow} \beta_o (\cos\beta_r - \cos\beta_o) = -(\beta_r - \beta_o)\sin\beta_o. \quad (44)$$

Similarly we have

$$\lim_{\beta_r \rightarrow \beta_o} (\sin\beta_r - \sin\beta_o) = (\beta_r - \beta_o)\cos\beta_o. \quad (45)$$

Substitution of equation 40 and 41 into equation 39 yields

$$T'_{23} = \lim_{\beta_r \rightarrow \beta_o} \left[\frac{1}{R_s(\beta_r - \beta_o)}\right]\{[(A+R_m)\cos\beta_s \cos\lambda_s - R_m \cos\beta_o \cos\lambda_o]\cos\lambda_o (\cos\beta_r - \cos\beta_o) + [(A+R_m)\cos\beta_s \sin\lambda_s - R_m \cos\beta_o \sin\lambda_o]\sin\lambda_o (\cos\beta_r - \cos\beta_o) + [(A+R_m)\sin\beta_s - R_m \sin\beta_o]\,(\sin\beta_r - \sin\beta_o)\}$$

In the limit (and from equations 44 and 45) this becomes

$$T'_{23} = \frac{(A+R_m)}{R_s}[\cos\beta_s \cos(\lambda_s - \lambda_o)\sin\beta_o - \sin\beta_s \cos\beta_o]. \quad (46)$$

Equations 37, 38, and 46 provide three (T'_{21}, T'_{33}, T'_{23}) of the nine elements of the transformation matrix. Properties of the elements of the transformation matrix are

$$T'^{2}_{11} + T'^{2}_{12} + T'^{2}_{13} = 1 \quad (47)$$

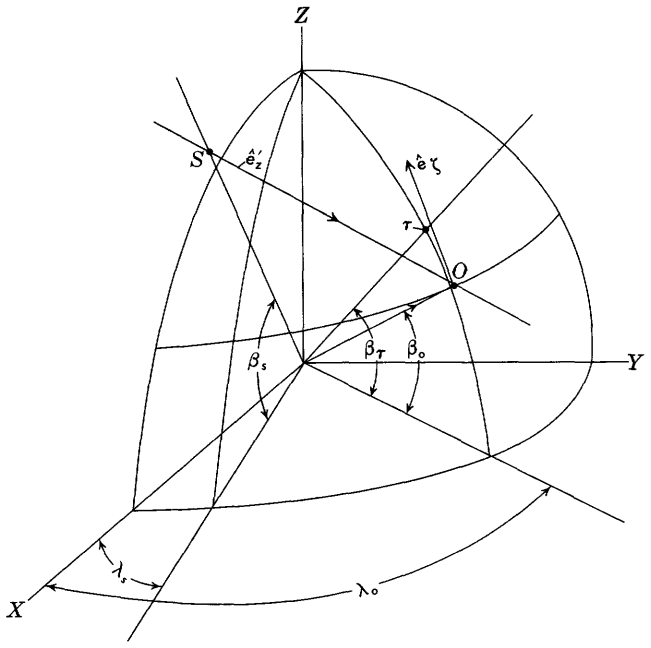

FIGURE 12.—Relationships between the $\hat{e}'_i$ vector and the $\hat{e}_\zeta$ vector.

$$T'^{\,2}_{21}+T'^{\,2}_{22}+T'^{\,2}_{23}=1 \tag{48}$$

$$T'^{\,2}_{31}+T'^{\,2}_{32}+T'^{\,2}_{33}=1 \tag{49}$$

$$T'_{11}T'_{12}+T'_{21}T'_{22}+T'_{31}T'_{32}=0 \tag{50}$$

$$T'_{11}T'_{13}+T'_{21}T'_{23}+T'_{31}T'_{33}=0 \tag{51}$$

$$T'_{12}T'_{13}+T'_{22}T'_{23}+T'_{32}T'_{33}=0 \tag{52}$$

Therefore, having evaluated three of the elements previously and having six independent equations defining the properties of the elements of the matrix, it is now possible to evaluate all nine elements of the transformation matrix.

From equation 48, since

$$T'_{21}=0 \text{ (equation 37)}$$

then

$$T'_{22}=\sqrt{1-T'^{\,2}_{23}}. \tag{53}$$

NOTE.—It is possible to express equations 47 through 49 in the form

$$T'^{\,2}_{13}+T'^{\,2}_{23}+T'^{\,2}_{33}=1.$$

This is not an independent equation but is implicit from equations 47 through 49. Therefore,

$$T'_{13}=\sqrt{1-T'^{\,2}_{33}-T'^{\,2}_{23}}. \tag{54}$$

Dividing equation 50 by equation 51 and noting that

$$T'_{21}=0 \text{ (equation 37)}$$

then

$$\frac{T'_{11}T'_{12}}{T'_{11}T'_{13}}=\frac{T'_{31}T'_{32}}{T'_{31}T'_{33}}$$

$$\therefore\ T'_{12}=T'_{13}\frac{T'_{32}}{T'_{33}}. \tag{55}$$

Substitution of equation 55 in equation 52 yields

$$T'_{32}=\frac{-T'_{22}T'_{23}}{\left(\frac{T'^{\,2}_{13}}{T'_{33}}+T'_{33}\right)}=-\frac{T'_{23}T'_{33}}{\sqrt{1-T'^{\,2}_{23}}}. \tag{56}$$

Using equations 54 and 56 in equation 55,

$$T'_{12}=-\sqrt{1-\frac{T'^{\,2}_{33}}{1-T'^{\,2}_{23}}}\,T'_{23}. \tag{57}$$

From equation 47, we obtain

$$T'_{11}=\sqrt{1-T'^{\,2}_{12}-T'^{\,2}_{13}},$$

which using equations 54 and 57 can be written as

$$T'_{11}=\frac{T'_{33}}{\sqrt{1-T'^{\,2}_{23}}}. \tag{58}$$

Using equations 49 and 56, this equation becomes

$$T'_{31}=\sqrt{1-\frac{T'^{\,2}_{33}}{(1-T'^{\,2}_{23})}}. \tag{59}$$

Thus, all nine elements of the T'_{ij} transformation matrix have now been evaluated. The elements are given by equations 37, 38, 46, 53, 54, 56, 57, 58, and 59. It is now possible to determine X_i from the X'_j coordinates.

Recall from equation 35

$$x_i = \sum_j T'_{ij} x''_j.$$

Therefore, if the coordinates x''_j (for $\xi = 0$) can be transformed from the x'_k coordinates (η' and ζ') the problem is finished. Referring to figure 10, we note that

$$\sum_j x''_j \hat{e}''_j = \sum_k x_k \hat{e}'_k.$$

Dotting $\hat{e}''_j$ into the equation above, we have

$$\sum_j \hat{e}''_j \cdot (x''_j \hat{e}''_j) = \sum_k \hat{e}''_j \cdot (x'_k \hat{e}'_k).$$

Noting that $\hat{e}''_j \cdot \hat{e}''_j = 1$, we obtain

$$x''_j = \sum_k (\hat{e}''_j \cdot \hat{e}'_k) x'_k = \sum_k T'''_{jk} x'_k$$

or

$$T_{jk} = \hat{e}''_j \cdot \hat{e}'_k. \tag{60}$$

Note the following:

1. In the $\xi = 0$ and x' systems, Z' is coincident,

$$\therefore T'''_{33} = 1. \tag{61}$$

2. Since η'' and ζ'' are perpendicular to the Z' axis,

$$T'''_{31} = T'''_{32} = 0 \tag{62a}$$

and

$$T'''_{13} = T'''_{23} = 0. \tag{62b}$$

Again referring to figure 10, we have

$$T'''_{22} = \hat{e}''_\zeta \cdot \hat{e}'_\zeta = \cos \xi \tag{63}$$

$$T'''_{11} = \cos \xi \tag{64}$$

$$T'''_{12} = \cos (90 + \xi) = -\sin \xi \tag{65}$$

$$T'''_{21} = \cos (90 - \xi) = \sin \xi \tag{66}$$

In matrix notation, we have

$$T'''_{jk} = \begin{vmatrix} \cos \xi & -\sin \xi & 0 \\ \sin \xi & \cos \xi & 0 \\ 0 & 0 & 1 \end{vmatrix}. \tag{67}$$

Then from definition,

$$x_i = \sum_j T'_{ij} x''_j$$

$$x''_j = \sum_k T'''_{jk} x'_k$$

$$\therefore x_i = \sum_{jk} T'_{ij} T'''_{jk} x'_k = \sum_k T_{ik} x'_k$$

or

$$\eta_p = m[T_{11}\eta'_p + T_{12}\zeta'_p + T_{13} Z'_p]$$

$$\zeta_p = m[T_{21}\eta'_p + T_{22}\zeta'_p + T_{23} Z'_p]$$

and

$$T_{ik} = \sum_j T'_{ij} T'''_{jk},$$

which in matrix notation is

$$T_{ik} = \begin{vmatrix} T'_{11} & T'_{12} & T'_{13} \\ T'_{21} & T'_{22} & T'_{23} \\ T'_{31} & T'_{32} & T'_{33} \end{vmatrix} \begin{vmatrix} \cos \xi & -\sin \xi & 0 \\ \sin \xi & \cos \xi & 0 \\ 0 & 0 & 1 \end{vmatrix}. \tag{68}$$

Listing the elements we have

$$T_{11} = \cos \xi \, T'_{11} + \sin \xi \, T'_{12}$$

$$T_{12} = -\sin \xi \, T'_{11} + \cos \xi \, T'_{12}$$

$$T_{13} = T'_{13}$$

$$T_{21} = \cos \xi \, T'_{21} + \sin \xi \, T'_{22}$$

$$T_{22} = -\sin \xi \, T'_{21} + \cos \xi \, T'_{22}$$

$$T_{23} = T'_{23}$$

$$T_{31} = \cos \xi \, T'_{31} + \sin \xi \, T'_{32}$$

$$T_{32} = -\sin\xi\, T'_{31} + \cos\xi\, T'_{32}$$

$$T_{33} = T'_{33}$$

Where the T'_{ij} elements are given in equations 37, 38, 46, 53, 54, 56, 57, 58, and 59. Making these substitutions, we obtain

$$T_{11} = \cos\xi \frac{T'_{33}}{\sqrt{1-T'^{2}_{23}}} - \sin\xi\, T'_{23} \sqrt{1-\frac{T'^{2}_{33}}{1-T'^{2}_{23}}} \tag{69}$$

$$T_{12} = -\sin\xi \frac{T'_{33}}{\sqrt{1-T'^{2}_{23}}} - \cos\xi\, T'_{23} \sqrt{1-\frac{T'^{2}_{33}}{1-T'^{2}_{23}}} \tag{70}$$

$$T_{13} = \sqrt{1-T'^{2}_{33}-T'^{2}_{23}} \tag{71}$$

$$T_{21} = \sin\xi \sqrt{1-T'^{2}_{23}} \tag{72}$$

$$T_{22} = \cos\xi \sqrt{1-T'^{2}_{23}} \tag{73}$$

$$T_{23} = T'_{23} \tag{74}$$

$$T_{31} = \cos\xi \sqrt{1-\frac{T'^{2}_{33}}{1-T'^{2}_{23}}} - \sin\xi \frac{T'_{23}T'_{33}}{\sqrt{1-T'^{2}_{23}}} \tag{75}$$

$$T_{32} = -\sin\xi \sqrt{\frac{(1-T'_{23})^2 - T'^{2}_{33}}{(1-T'_{23})^2}} - \cos\xi \frac{T'_{23}T'_{33}}{\sqrt{1-T'^{2}_{33}}} \tag{76}$$

$$T_{33} = T'_{33} \tag{77}$$

It is now possible to compute η_p and ζ_p using equations 32 and 33 and thus the slope. A summary of the equations to be used in calculating the slope follows.

SUMMARY OF THE PROCEDURE TO COMPUTE THE SLOPE

This section is presented to encourage the eventual programing of the technique developed in this paper. The summary is therefore arranged in the order in which a computer program would be written.

1. From the support data we have the following parameters:

   R_m Radius of moon, constant.

   R_s Slant range along optic axis to intercept with surface.

   A Spacecraft altitude.
   β_s, λ_s Latitude and longitude of spacecraft.
   $\beta_\odot, \lambda_\odot$ Latitude and longitude of subsolar point.
   β_o, λ_o Latitude and longitude of optic axis intercept with surface.

2. Determine the values of T'_{23} and T'_{33}.
   From equation 46,

$$T'_{23} = \frac{(A+R_m)}{R_s}\left[\cos\beta_s \cos(\lambda_s-\lambda_o)\sin\beta_o - \sin\beta_s \cos\beta_o\right]$$

   and from equation 38,

$$T'_{33} = \frac{1}{2}\left[\frac{R_s}{R_m} - \frac{A}{R_s}\left(\frac{A}{R_m}+2\right)\right].$$

3. Determine ξ, η'_p, ζ'_p from the photograph.
4. Generate the transformation matrix

$$T_{ij} = f(T'_{33}, T'_{23}, \xi),$$

   whose elements are given in equations 69 through 77:

$$T_{11} = \cos\xi \frac{T'_{33}}{\sqrt{1-T'^{2}_{23}}} - \sin\xi\, T'_{23} \sqrt{1-\frac{T'^{2}_{33}}{1-T'^{2}_{23}}}$$

$$T_{12} = -\sin\xi \frac{T'_{33}}{\sqrt{1-T'^{2}_{23}}} - \cos\xi\, T'_{23} \sqrt{1-\frac{T'^{2}_{33}}{1-T'^{2}_{23}}}$$

$$T_{13} = \sqrt{1-T'^{2}_{33}-T'^{2}_{23}}$$

$$T_{21} = \sin\xi \sqrt{1-T'^{2}_{23}}$$

$$T_{22} = \cos\xi \sqrt{1-T'^{2}_{23}}$$

$$T_{23} = T'_{23}$$

$$T_{31} = \cos\xi \sqrt{1 - \frac{T'^{2}_{33}}{1 - T'^{2}_{23}}} - \sin\xi \frac{T'_{23} T'_{33}}{\sqrt{1 - T'^{2}_{23}}}$$

$$T_{32} = -\sin\xi \sqrt{\frac{(1 - T'_{23})^2 - T'^{2}_{33}}{(1 - T'_{23})^2}} - \cos\xi \frac{T'_{23} T'_{33}}{\sqrt{1 - T'^{2}_{23}}}$$

$$T_{33} = T'_{33}$$

5. Determine the brightness from the density data and the H and D curve.
6. Using η'_p and ζ'_p determine g, α, and ψ.
   (a) To determine g, we use equation 9.

$$\cos g = \frac{\left(1 + \frac{A}{R_m}\right)\left\{[\cos\beta \cos\beta_s \cos(\lambda_s - \lambda_\odot) + \sin\beta_\odot \sin\beta_s] - [\cos\beta \cos\beta_p \cos(\lambda_p - \lambda_\odot) + \sin\beta_\odot \sin\beta_p]\right\}}{\left\{\left(1 + \frac{A}{R_m}\right)^2 + 1 - 2\left(1 + \frac{A}{R_m}\right)[\cos\beta_s \cos\beta_p \cos(\lambda_s - \lambda_p) + \sin\beta_s \sin\beta_p]\right\}^{1/2}}$$

where β_p, λ_p are the latitude and longitude of an arbitrary point of interest on the lunar surface and are determined from equations 21 and 22.

$$\therefore \lambda_p = \frac{\eta_p}{R_m \cos\beta_o} + \lambda_o$$

$$\beta_p = \beta_o - \frac{\zeta_p}{R_m}$$

η_p and ζ_p can be determined from equations 32 and 33.

$$\eta_p = m[(T_{11} + T_{13}KT_{31})\eta'_p + (T_{12} + T_{13}KT_{32})\zeta'_p]$$

$$\zeta_p = m[(T_{21} + T_{23}KT_{31})\eta'_p + (T_{22} + T_{23}KT_{32})\zeta'_p]$$

where

$$K = \frac{T_{33}(\sqrt{1 - T^2_{33}} - 1)}{\sqrt{1 - T^2_{33}}\,(1 - T^2_{33})}$$

   (b) To determine α, we use g and the brightness value.
   (c) Using α, we now determine the slope from equation 16.

$$\sin\psi = -[\sin(g - \alpha) + \cot g \cos(g - \alpha)]\,\hat{v}_\odot \cdot \hat{v}_p + \left[\frac{\cos(g - \alpha)}{\sin g}\right]\hat{v}_{ps} \cdot \hat{v}_p,$$

where $\hat{v}_\odot \cdot \hat{v}_p$ and $\hat{v}_{ps} \cdot \hat{v}_p$ are determined from equations 17 and 20.

$$\therefore \hat{v}_\odot \cdot \hat{v}_p = \cos\beta_\odot \cos\beta_p \cos(\lambda_\odot - \lambda_p) + \sin\beta_\odot \sin\beta_p$$

$$\hat{v}_{ps} \cdot \hat{v}_p = \frac{\left\{\left[\left(1 + \frac{A}{R_m}\right)\cos\beta_p \cos\beta_s \cos(\lambda_s - \lambda_p) + \sin\beta_p \sin\beta_s\right] - 1\right\}}{\left\{\left(1 + \frac{A}{R_m}\right)^2 + 1 - 2\left(1 + \frac{A}{R_m}\right)[\cos\beta_s \cos\beta_p \cos(\lambda_s - \lambda_p) + \sin\beta_s \sin\beta_p]\right\}^{1/2}}$$

Using the equations summarized in this section, it is now possible to compute the slope component of the surface in the phase plane.

CONCLUSIONS

A new generalized derivation of an operational technique for extracting terrain slope information from planetary surfaces photometrically has been developed. The solution is in a general form and can be applied to an analysis of either vertical or oblique photography. Although the solution is intended primarily for deriving topographic data for the lunar surface, it can also be applied to obtain information about other planetary surfaces if used within the limitations of the basic assumptions.

During the derivation the authors made two assumptions: (1) the mean lunar surface is flat

rather than spherical over the area of interest, and (2) distances on lunar surface were small as compared to the radius of the moon.

Finally, the summary of equations should serve as a useful tool to those interested in adapting the technique to a digital computer.

SELECTED REFERENCES

Coburn, Nathaniel, 1955, Vector and tensor analysis [1st ed.]: N.Y., Macmillan Co., 341 p.

Dale, E. D., 1962, The application of the van Diggelen method of slope analysis to lunar domes and wrinkle ridges: Manchester, England, University of Manchester, Thesis, p. 46.

Diggelen, J. van, 1951, A photometric investigation of the slopes and heights of the ranges of hills in the maria of the moon: Netherland Astron. Inst. Bull., v. 11, p. 283–289.

——— 1959, Photometric properties of lunar crater floors: Utrecht Observatory Recherches Astronomy, v. 14, no. 2, 114 p.

Hapke, B. W., 1963, A theoretical photometric function for the lunar surface: Jour. Geophys. Research, v. 68, no. 15, 4571–4586.

——— 1966, An improved theoretical lunar photometric function: Astron. Jour., v. 71, no. 5, p. 33–339.

Herriman, A., Washburn, H., and Willingham, D., 1963, Ranger preflight analysis and the lunar photometric model: California Inst. Technology Jet Propulsion Lab. Tech. Report 32–384.

Kaplan, Wilfred, 1959, Advanced calculus [5th ed.]: Reading, Mass., Addison-Wesley Pub. Co., Inc.

McCauley, J. F., 1965, Terrain analysis of the lunar equatorial belt: U.S. Geol. Survey open-file report, 44 p.

Minnaert, M., 1961, Photometry of the Moon, *in* Kuiper, G. P., and Middlehurst, B. M., eds., Planets and satellites, v. 3 *of* The solar system: Chicago Univ. Press, p. 213–245.

Watson, Kenneth, 1968, Photoclinometry from spacecraft images: U.S. Geol. Survey Prof. Paper 599–B, 10 p.

Wildey, R. L., and Pohn, H. A., 1964, Detailed photoelectric photometry of the Moon: Astron. Jour., v. 69, no. 8, p. 619–634.

Wilhelms, D. E., 1963, A photometric technique for measurement of lunar slopes: Studies for space flight program: Astrogeol. Studies Ann. Progress Report, August 1962 to July 1963, U.S. Geol. Survey open-file report, p. 1–12.

Willingham, D., 1964, The lunar reflectivity model for Ranger block III analysis: California Inst. Technology Jet Propulsion Lab. Tech. Report 32–664.

* U.S. GOVERNMENT PRINTING OFFICE: 1973—543–576/12